Chemistry–A European Journal
Research Article
doi.org/10.1002/chem.202300709
Chemistry Europe
European Chemical Societies Publishing
www.chemeurj.org

Assembling Artificial Photosynthetic Models in Water Using β-Cyclodextrin-Conjugated Phthalocyanines as Building Blocks

Xiao-Fei Chen,[a, b] Habtom B. Gobeze,[c] Francis D'Souza,*[c] and Dennis K. P. Ng*[a]

Abstract: Two water-soluble zinc(II) phthalocyanines substituted with two or four permethylated β-cyclodextrin (β-CD) moieties at the α positions have been utilized as building blocks for the construction of artificial photosynthetic models in water. The hydrophilic and bulky β-CD moieties not only can increase the water solubility of the phthalocyanine core and prevent its stacking in water but can also bind with a tetrasulfonated zinc(II) porphyrin (ZnTPPS) and/or sodium 2-anthraquinonesulfonate (AQ) in water through host–guest interactions. The binding interactions of these species have been studied spectroscopically, while the photoinduced processes of the resulting complexes have been investigated using steady-state and time-resolved spectroscopic methods. In the ternary complexes, the ZnTPPS units serve as light-harvesting antennas to capture the light energy and transfer it to the phthalocyanine core via efficient excitation energy transfer. The excited phthalocyanine is subsequently quenched by the electron-deficient AQ units through electron transfer. Femtosecond transient absorption spectroscopy provides clear evidence for the singlet-singlet energy transfer from the photo-excited ZnTPPS to the phthalocyanine core with a rate constant (k_{ENT}) in the order of $10^9\ s^{-1}$. The population of phthalocyanine radical cations indicates the occurrence of electron transfer from the excited phthalocyanine to the AQ moieties, forming a charge-separated state.

Introduction

In nature, photosynthetic organisms utilize solar energy as an abundant resource.[1] Through a series of photoinduced processes, they convert sunlight into chemical energy, producing essential materials for their growth. This fascinating process has inspired researchers to develop artificial counterparts that can mimic the light-harvesting, charge-separation, and multi-electron catalytic processes in photosynthesis.[2] These studies are fundamentally important in the exploitation of sustainable and environmentally benign solar fuels to meet energy demands.[3] To construct these artificial photosynthetic models, a variety of chromophores and redox-active species have been utilized as functional components.[4] These molecular components are connected through different means and skeletons and are immobilized on different platforms with a view to envisioning the factors governing the photoinduced energy and electron transfer processes and optimizing the light-conversion efficiency.[5] Through extensive studies, considerable progress has been made in this field over the years.

Among the various functional units, porphyrins are probably the most commonly used components in artificial photosynthetic models because of their biological relevance, ease of chemical modification, and rich optical and redox properties.[4a,d–f] With high versatility and many advantageous properties as porphyrins, phthalocyanines are also promising candidates for the construction of these models, particularly as light-harvesting chromophores and electron donors.[4a,e,6] We have previously reported a series of silicon(IV) phthalocyanines connected covalently[7] or non-covalently[8] to porphyrins to study their photoinduced processes. The models held by host–guest interactions of silicon(IV) phthalocyanines substituted axially with two permethylated β-cyclodextrin (β-CD) moieties and tetrasulfonated porphyrins are of particular interest.[8a,c–e] This supramolecular approach not only enables the assembly of artificial photosynthetic models in aqueous media, which are relatively rare,[9] but also facilitates the construction process through self-assembly. As an extension of these studies, we report herein the self-assembly of two zinc(II) phthalocyanines substituted with two or four permethylated β-CD moieties at

[a] Dr. X.-F. Chen, Prof. D. K. P. Ng
Department of Chemistry
The Chinese University of Hong Kong
Shatin, N.T., Hong Kong (China)
E-mail: dkpn@cuhk.edu.hk
Homepage: https://chem.cuhk.edu.hk/people/academic-staff/nkp/
[b] Dr. X.-F. Chen
Guangdong Provincial Key Laboratory of Chemical Measurement and Emergency Test Technology, Institute of Analysis
Guangdong Academy of Sciences
(China National Analytical Center, Guangzhou)
Guangzhou 510070 (China)
[c] Dr. H. B. Gobeze, Prof. F. D'Souza
Department of Chemistry
University of North Texas
Denton, TX 76201 (USA)
E-mail: francis.dsouza@unt.edu
Homepage: https://chemistry.unt.edu/people-node/francis-dsouza

Supporting information for this article is available on the WWW under https://doi.org/10.1002/chem.202300709

the α positions (compounds **1** and **2**), a tetrasulfonated zinc(II) porphyrin (ZnTPPS), and sodium 2-anthraquinonesulfonate (AQ) in water and the study of the photoinduced energy and electron transfer processes of the resulting host–guest complexes using a range of steady-state, time-resolved, and transient absorption spectroscopic methods. The molecular structures of these host and guest species are shown in Figure 1.

Results and Discussion

Complexation with ZnTPPS

The β-CD-substituted phthalocyanines **1** and **2** were prepared according to our previously reported procedure.[10] With bulky and hydrophilic β-CD moieties at the α positions of the phthalocyanine core, these compounds were found to be soluble in water and remain essentially non-aggregated in aqueous media as shown by their sharp and intense Q-band absorption (Figure S1). These properties are essential for components in artificial photosynthetic models as stacking of hydrophobic molecules, which is highly favorable in aqueous media, would provide an efficient alternative relaxation pathway for the excited species, greatly affecting the photoinduced processes.

We first studied the complexation of these host species with ZnTPPS in water using electronic absorption and fluorescence spectroscopic methods. As shown in Figure 2a, upon addition of **1** (from 0 to 4 μM), the Soret band of ZnTPPS (2 μM) at 421 nm was slightly red-shifted to 424 nm, while the absorption bands of **1** at 342 and 692 nm were virtually unshifted. By plotting the change in absorbance at 421 and 424 nm versus the concentration ratio of **1** to ZnTPPS (Figure 2b), it was found that the change became negligible when more than one equiv. of **1** was added. Upon selective excitation of ZnTPPS at 550 nm, where **1** showed negligible absorption (Figure S1), a pair of fluorescence bands at 605 and 656 nm of ZnTPPS were observed. Upon addition of **1**, these two bands were diminished, while a new emission band at 706 nm appeared, which could be assigned to the fluorescence of **1** (Figure 2c). In the excitation spectrum (monitored at 706 nm) of a 1 : 1 mixture of these two compounds (Figure S2), apart from the bands associated with the absorptions of **1** (at ca. 350, 610, and 690 nm), a strong band at ca. 420 nm and a weak signal at ca. 550 nm were also observed, which could be assigned to the absorptions of ZnTPPS. These results strongly suggested the occurrence of excitation energy transfer (EET) from the excited ZnTPPS to **1**. By examining the extent of quenching of the fluorescence of ZnTPPS upon complexation with **1** (Figure S3), the EET efficiency was estimated to be 84%. Job's plot analysis of the fluorescence data revealed a 1 : 1 binding stoichiometry (Figure 2d), which was consistent with the results depicted in

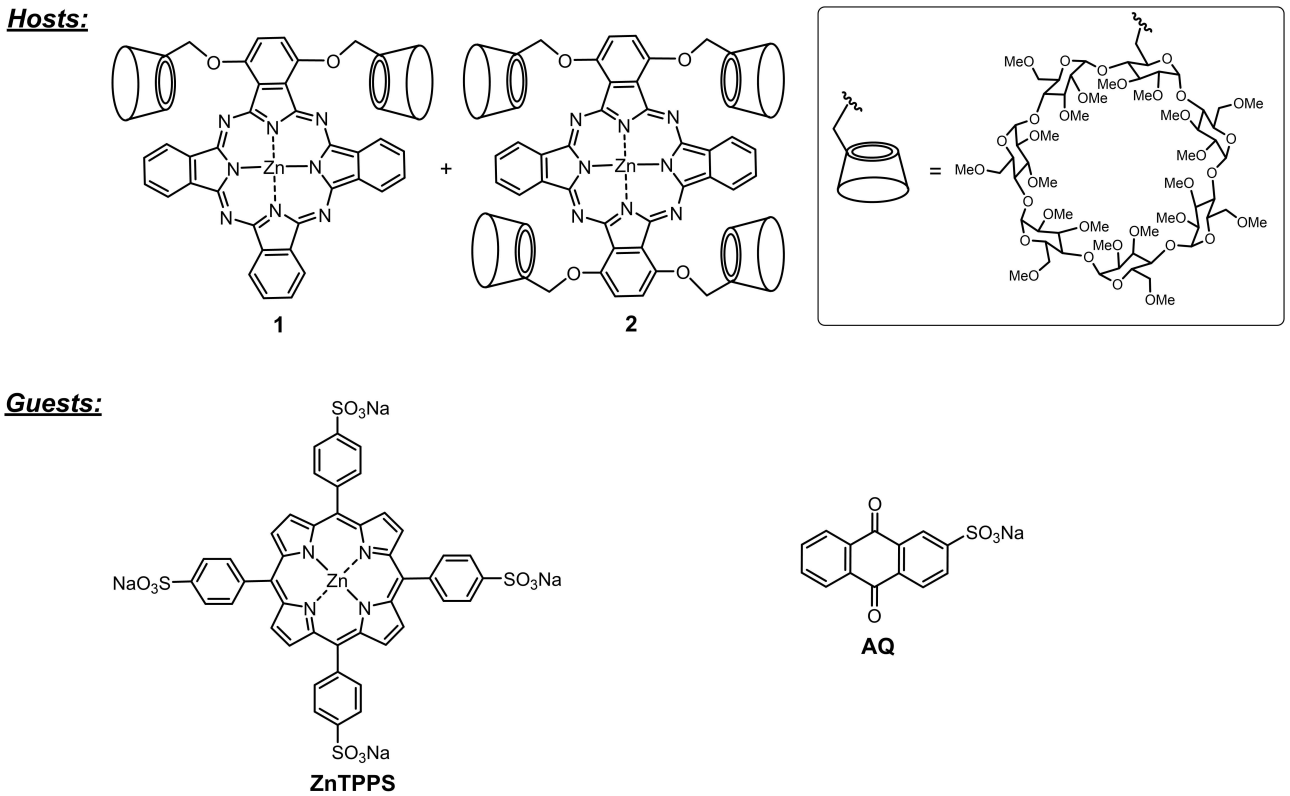

Figure 1. Molecular structures of β-CD-substituted phthalocyanines **1** and **2** as the host species and ZnTPPS and AQ as the guest species for the construction of artificial photosynthetic models in water.

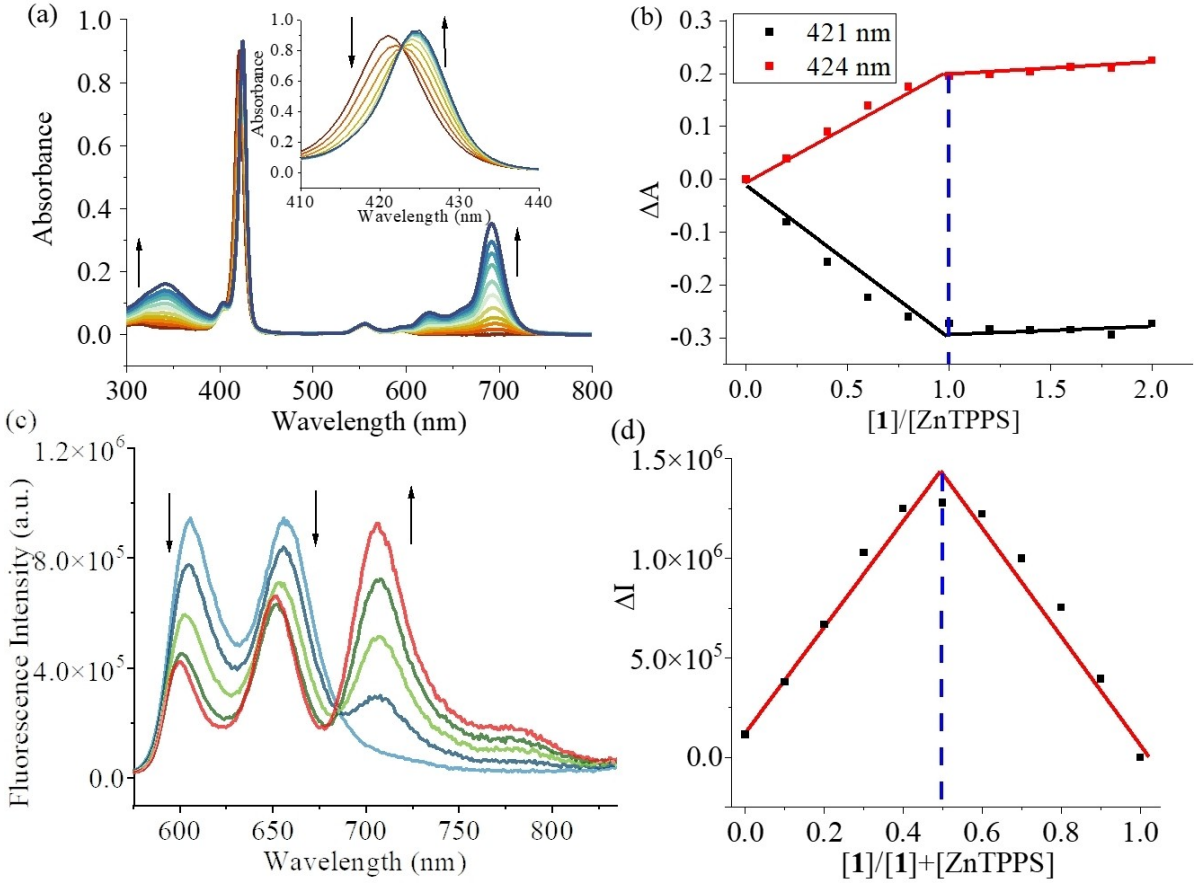

Figure 2. (a) Change in the electronic absorption spectrum of ZnTPPS (2 μM) upon the addition of **1** (from 0 to 4 μM) in water. The inset shows the enlarged region of the porphyrin's Soret band. (b) Change in the absorbance at 421 and 424 nm at different concentration ratios of **1** to ZnTPPS. (c) Change in the fluorescence spectrum of ZnTPPS (2 μM) upon the addition of **1** (from 0 to 4 μM) in water (λ_{ex} = 550 nm). (d) Job's plot for determination of the binding stoichiometry between **1** and ZnTPPS by monitoring the fluorescence intensity at 706 nm. The total concentration of **1** and ZnTPPS was fixed at 10 μM.

Figure 2b based on the absorption data. This binding stoichiometry was expected as meso-tetraarylporhyrins generally bind with β-CDs in a 1:2 manner[11] and **1** contains two β-CD moieties in a molecule.

The complexation between the tetrakis-β-CD analogue **2** and ZnTPPS was also studied similarly. As shown in Figure 3a, the Soret band of ZnTPPS (2 μM) was also slightly red-shifted from 421 to 424 nm upon the addition of **2** (from 0 to 2 μM). The absorbance at these two positions was not significantly changed further when more than 0.5 equiv. of **2** was added (Figure 3b), which suggested a 1:2 binding stoichiometry. The emerging peaks at 342 and 723 nm were due to the B- and Q-band absorptions of **2**, respectively. The latter was significantly red-shifted compared with that of **1** (at 692 nm) as a result of the two additional α substituents. Upon excitation of ZnTPPS at 550 nm, a pair of fluorescence bands at 605 and 656 nm of ZnTPPS were largely diminished with a concomitant increase in the fluorescence intensity at 730 nm upon the addition of **2** (Figure 3c). Again, this observation together with the appearance of the signals at ca. 420 and 550 nm assignable to ZnTPPS in the excitation spectrum of a 1:2 mixture of **2** and ZnTPPS (Figure S4) suggested the presence of EET. By comparing the fluorescence intensity of ZnTPPS before and after the addition of 0.5 equiv. of **2**, the EET efficiency was estimated to be 93% (Figure S5). The 1:2 binding stoichiometry was further supported by Job's plot analysis of the fluorescence data (Figure 3d).

As mentioned above, charged meso-tetraarylporphyrins usually bind with β-CDs in a 1:2 manner at the opposite meso positions in aqueous media (Figure 4a).[11] Owing to the strong host–guest interactions, the binding constants between the host and guest species are in the order of 10^4 M^{-1} for both K_1 and K_2 for the formation of the 1:1 and 1:2 complexes, respectively, or even higher, forming very stable supramolecular complexes.[11b] Based on this binding fashion and the determined binding stoichiometry, it is possible that ZnTPPS binds with **1** and **2** either in a discrete form as shown in Figure 4b or in a polymeric form as shown in Figure 4c. The formation of a 2:2 molecular wedge from a β-CD dimer and a tetrasulfonated porphyrin has been proposed previously.[12] To shed light on the possible binding mode of these species, transmission electron microscopy (TEM) was used to examine the morphology of the two mixtures. As shown in Figure S6, a fibrous morphology was observed for both complexes, which sug-

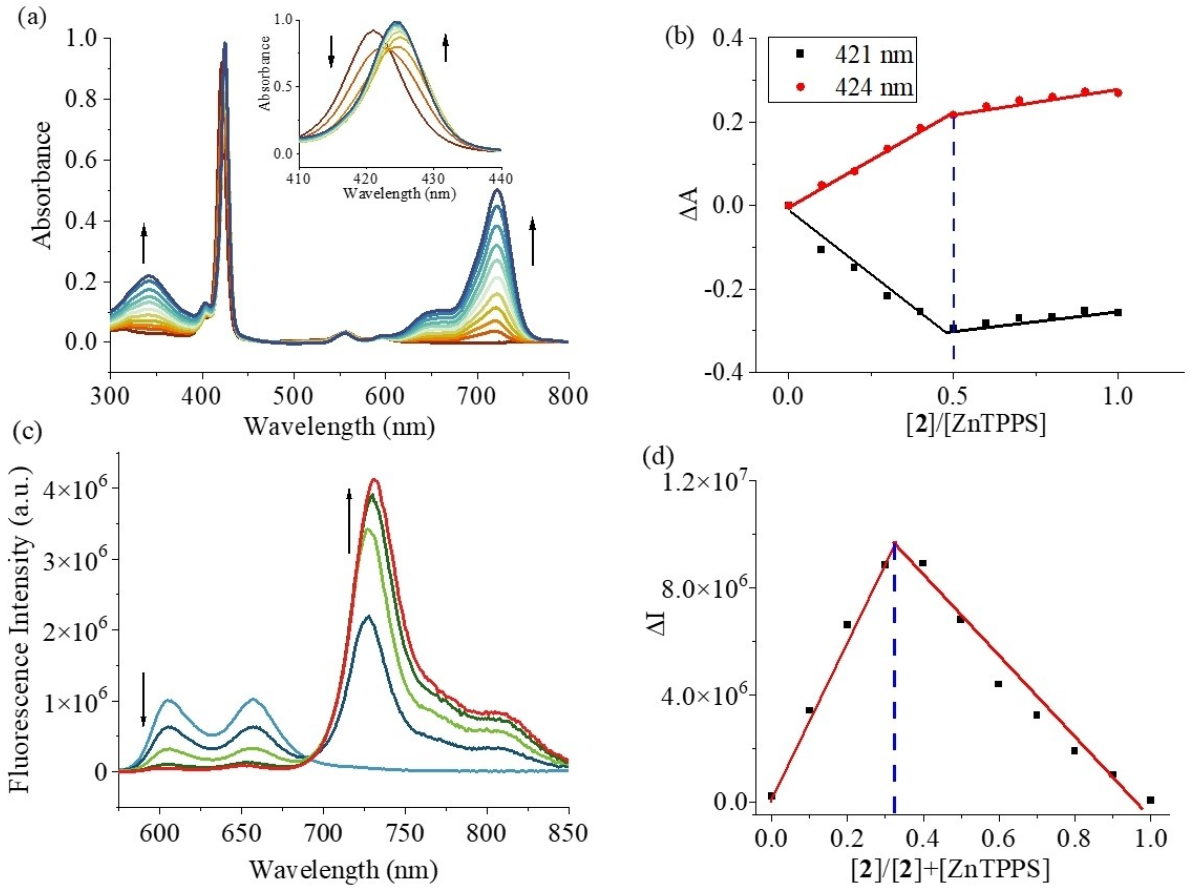

Figure 3. (a) Change in the electronic absorption spectrum of ZnTPPS (2 μM) upon the addition of **2** (from 0 to 2 μM) in water. The inset shows the enlarged region of the porphyrin's Soret band. (b) Change in the absorbance at 421 and 424 nm at different concentration ratios of **2** to ZnTPPS. (c) Change in the fluorescence spectrum of ZnTPPS (2 μM) upon the addition of **2** (from 0 to 2 μM) in water (λ_{ex} = 550 nm). (d) Job's plot for determination of the binding stoichiometry between **2** and ZnTPPS by monitoring the fluorescence intensity at 730 nm. The total concentration of **2** and ZnTPPS was fixed at 10 μM.

gested the preferential formation of a wire-like polymeric assembly (Figure 4c).

Complexation with AQ

The binding interactions of **1** and **2** with AQ in water were then studied in a similar manner. For the bis(β-CD) conjugate **1** (2 μM), both the Q-band absorption and the fluorescence intensity diminished upon the addition of AQ (from 0 to 8 μM) (Figure 5a, b). When 4 equiv. of AQ was added, the fluorescence intensity of **1** was quenched by 38%, which could be attributed to the photoinduced electron transfer (PeT) process from the excited **1** to the electron-accepting AQ moieties. A Job's plot analysis of the fluorescence data revealed a 1:2 binding stoichiometry (Figure 5c), suggesting simple inclusion of AQ into each of the β-CD moieties of **1**. The binding constant was determined to be 6.64×10^{11} M^{-2} by a linear least-squares fitting method[13] (Figure 5d), with an average of 8.15×10^{5} M^{-1} per β-CD/AQ unit, which was comparable with that of other β-CD-quinone complexes reported previously.[14]

Likewise, the Q-band absorption of **2** (2 μM) at 723 nm was also diminished along with the addition of AQ (from 0 to 16 μM) in water (Figure 6a). It was accompanied by a slightly intensified and blue-shifted B-band absorption (from 320 to 342 nm). The fluorescence band of **2** was also diminished, and the intensity was reduced by ca. 50% when 8 equiv. of AQ was added (Figure 6b). The quenching or PeT efficiency was slightly higher than that for **1** probably due to the presence of two additional β-CD moieties in **2**. As expected, **2** and AQ bind in a 1:4 fashion as revealed by the Job's plot analysis (Figure 6c). The binding constant was determined to be 3.48×10^{21} M^{-4} by a modified Benesi–Hildebrand equation[15] with an average of 2.43×10^{5} M^{-1} per β-CD/AQ unit (Figure 6d).

Excitation Energy and Electron Transfer Processes of the Host–Guest Complexes

The photoinduced processes of the supramolecular assemblies of **1** and **2** with ZnTPPS and AQ were then studied in water using various spectroscopic methods. We first prepared a mixture of **1** (2 μM) and ZnTPPS (1 μM) in water, under which

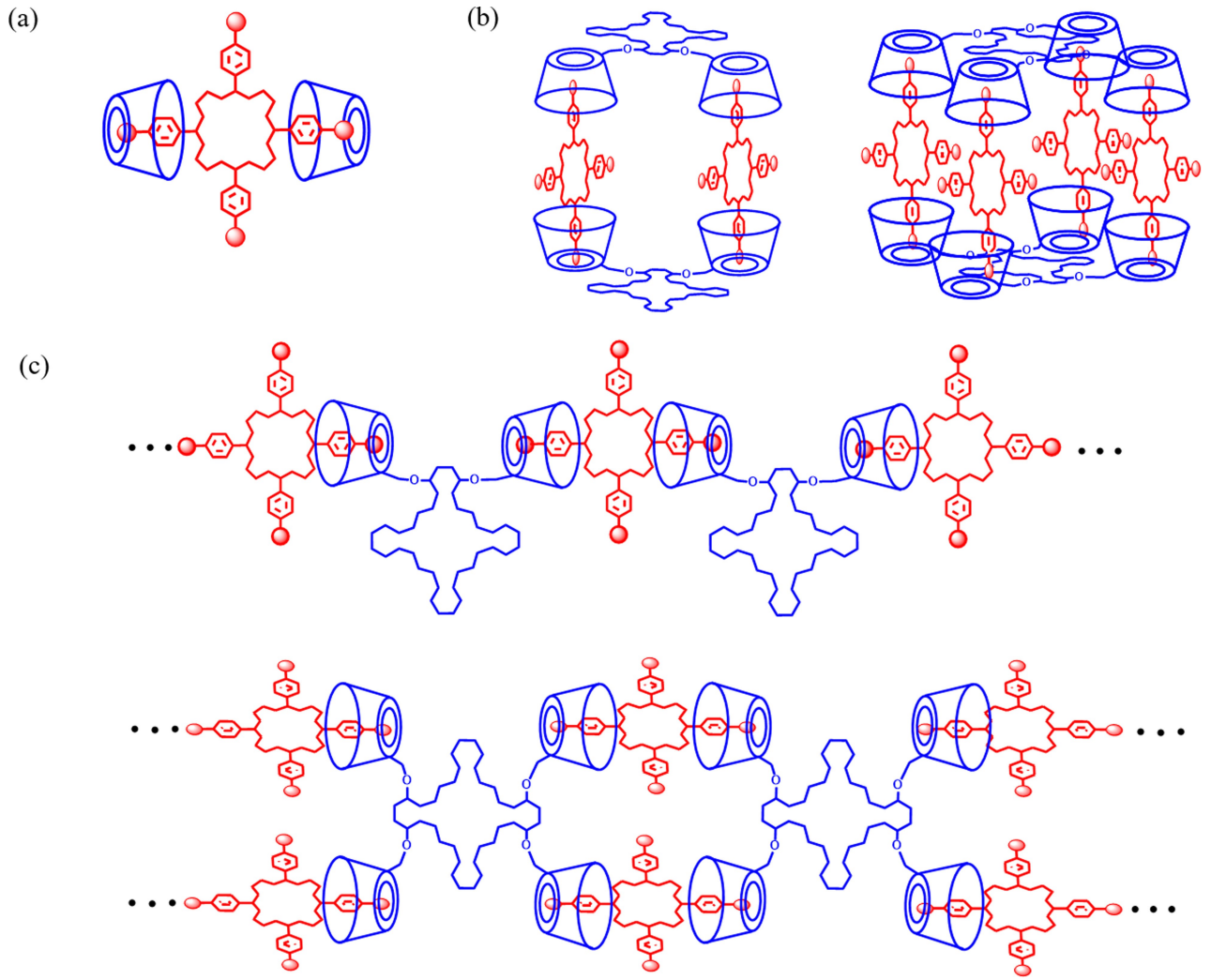

Figure 4. Schematic diagrams showing (a) a *trans*-type 1 : 2 complex of a charged meso-tetraarylporphyrin and a β-CD and the possible (b) discrete and (c) polymeric binding modes of ZnTPPS and **1** or **2**.

half of the β-CD binding sites would be occupied. Its absorption and fluorescence ($\lambda_{ex} = 550$ nm) spectra were monitored upon the addition of AQ (from 0 to 8 μM) (Figure S7). It is believed that under these conditions, dynamic ternary complexes of **1**, ZnTPPS, and AQ held by β-CD-based host–guest interactions were formed. Both the Q-band absorption of **1** and the fluorescence band at 705 nm assignable to this species were reduced in intensity gradually. The latter clearly showed the presence of sequential EET from the excited ZnTPPS to **1**, followed by PeT to the bound AQ. Similar results were obtained for a mixture of **2** (2 μM) and ZnTPPS (2 μM) in water upon the addition of up to 16 μM of AQ (Figure S8).

These photoinduced processes were then studied with time-resolved fluorescence spectroscopy. Upon excitation of **1** at 630 nm, the fluorescence decay at 710 nm could be fitted with an exponential function, giving a lifetime of 2.76 ns for the singlet excited state of **1** (Figure S9a). In the presence of 1 equiv. of ZnTPPS, the lifetime (2.81 ns) was not significantly changed. In the presence of 4 equiv. of AQ, the decay profile could be fitted with a two-exponential function, giving two lifetimes at 2.71 ns and 1.13 ns. The shorter lifetime was assumed to be associated with the charge separation between the excited **1** and AQ. However, the relative amplitude of this component was very small (only 4%), showing that the contribution of this charge-separated species, if present, was not significant. Similarly, for a mixture of **1**, ZnTPPS, and AQ (in a mole ratio of 1:0.5:2), the decay profile of the fluorescence intensity at 710 nm also led to two lifetimes at 2.75 ns and 1.48 ns with a relative amplitude of 95% and 5%, respectively. These results suggested that both ZnTPPS and AQ did not significantly perturb the singlet excited state of **1** under these conditions.

Similar results were also obtained for **2** by monitoring its time-dependent fluorescence intensity at 730 nm, both in the absence and presence of ZnTPPS and AQ (Figure S9b). For a mixture with 8 equiv. of AQ, the relative amplitude of the shorter-lifetime component was increased to 18%. Based on

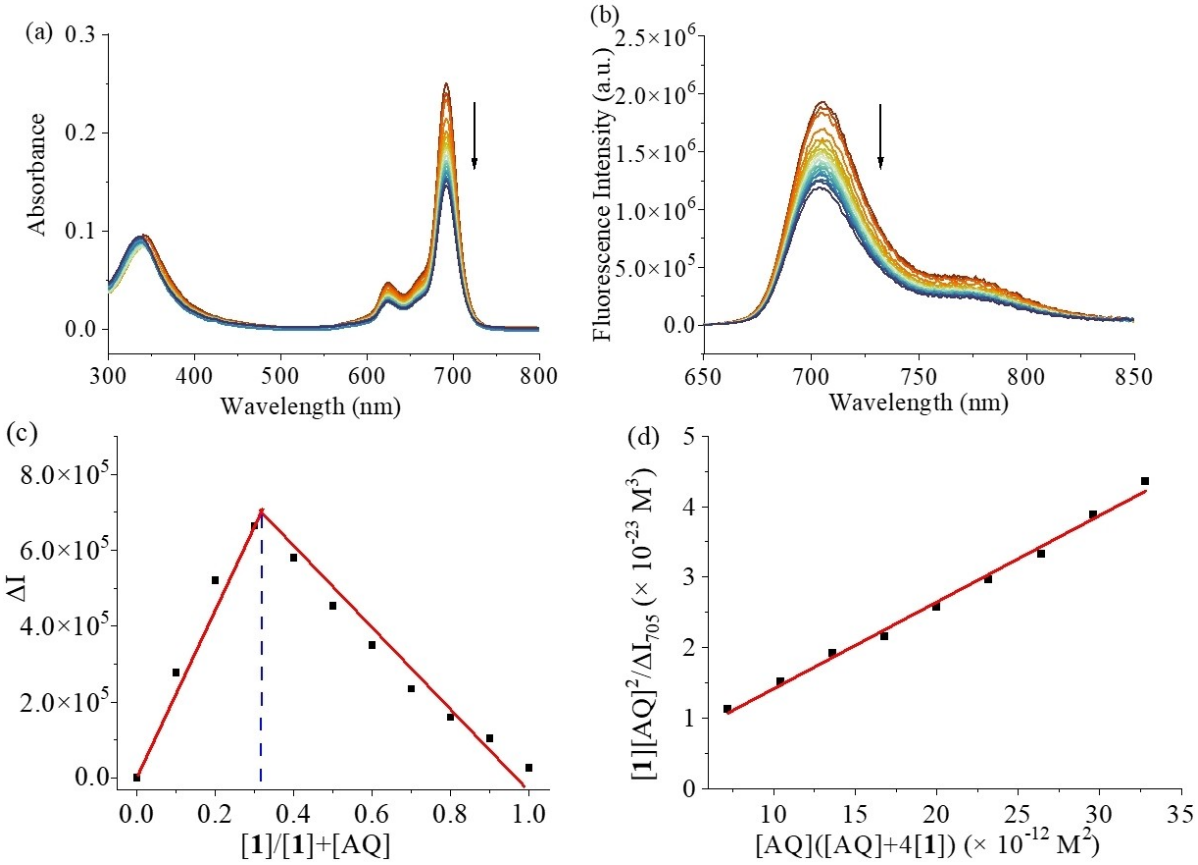

Figure 5. Change in the (a) electronic absorption and (b) fluorescence (λ_{ex} = 623 nm) spectra of **1** (2 μM) upon the addition of AQ (from 0 to 8 μM) in water. (c) Job's plot for determination of the binding stoichiometry between **1** and AQ by monitoring the fluorescence intensity at 705 nm. The total concentration of **1** and AQ was fixed at 10 μM. (d) A linear least-squares analysis plot for determination of the binding constant of **1** and AQ.

the two resolved lifetimes (1.98 ns and 0.74 ns), the rate of charge separation could be determined using Equation (1):

$$k_{CS} = \frac{1}{\tau_{(short)}} - \frac{1}{\tau_{(ref)}} \quad (1)$$

in which $\tau_{(short)}$ is the shorter lifetime caused by electron transfer and $\tau_{(ref)}$ is the lifetime of the reference compound without charge separation. The value for the complex of **2** and AQ was found to be 8.4×10^8 s^{-1}. For a mixture of **2**, ZnTPPS, and AQ (in a mole ratio of 1 : 0.5 : 4), two lifetimes (2.26 ns and 1.31 ns) were resolved with an amplitude ratio of 53 : 47, giving a rate of charge separation of 3.2×10^8 s^{-1}. All these data are summarized in Table 1.

Femtosecond transient absorption spectroscopy was then used to provide further insight into the excited-state interactions of the different components in the supramolecular assemblies. The spectra of **1**, **2**, and ZnTPPS were first recorded in deaerated water separately. Upon excitation with a femtosecond laser pulse at 650 nm, the differential absorption spectra of **1** were dominated by instantaneous formation of a pronounced bleaching at 694 nm and positive signals in the visible (450–620 nm) and near-infrared (800–1200 nm) regions. The former was due to the ground-state bleaching (GSB) and

Table 1. Fluorescence lifetimes of **1**, **2**, and their host–guest complexes with ZnTPPS and AQ in water.[a]

Complex	τ [ns]/Rel. Amp. [%]	Rate of Charge Separation [s^{-1}]
1	2.76 (100)	
1 + ZnTPPS (1 equiv.)	2.81 (100)	
1 + AQ (4 equiv.)	2.71 (96), 1.13 (4)	
1 + ZnTPPS (0.5 equiv.) + AQ (2 equiv.)	2.75 (95), 1.48 (5)	
2	1.90 (100)	
2 + ZnTPPS (2 equiv.)	1.86 (100)	
2 + AQ (8 equiv.)	1.98 (82), 0.74 (18)	8.4×10^8
2 + ZnTPPS (0.5 equiv.) + AQ (4 equiv.)	2.26 (53), 1.31 (47)	3.2×10^8

[a] Excited with a 630 nm laser and monitored at 710 (for **1**) or 730 (for **2**) nm. The concentrations of **1** and **2** were both 2 μM.

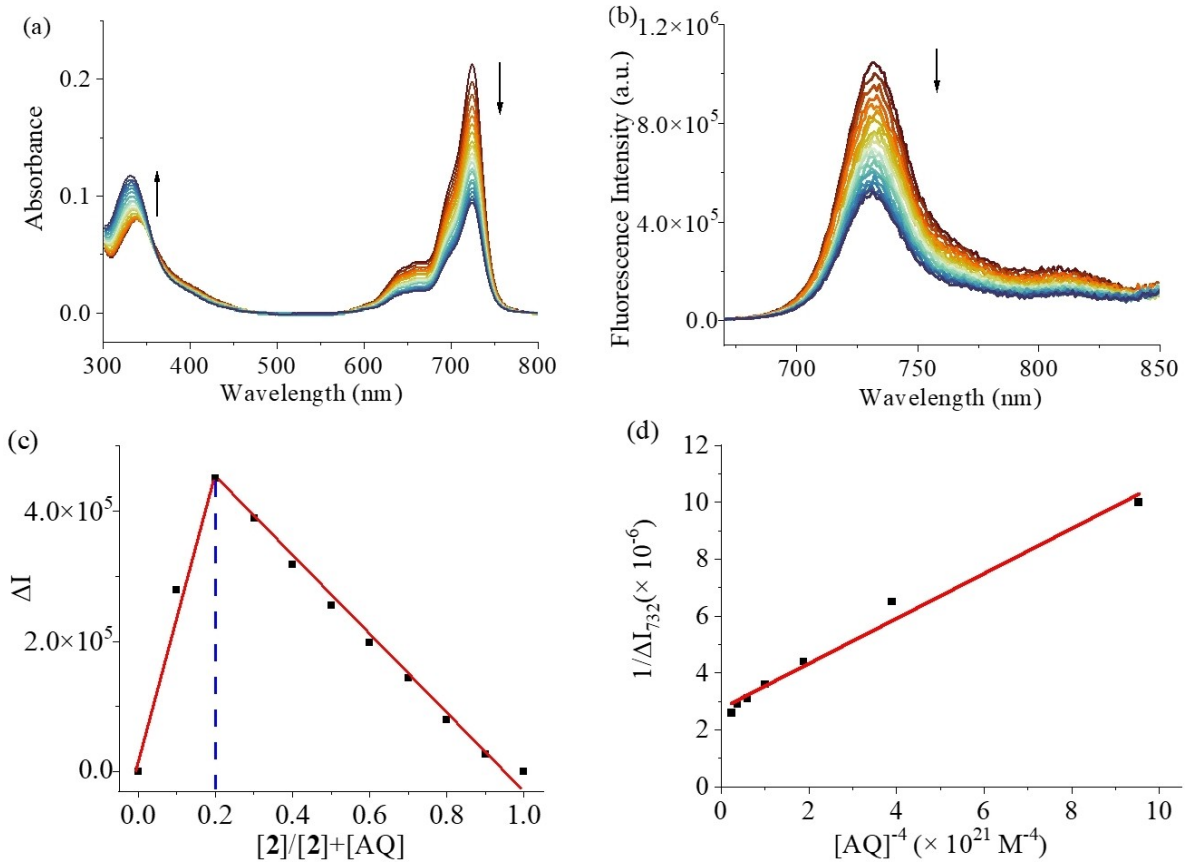

Figure 6. Change in the (a) electronic absorption and (b) fluorescence (λ_{ex} = 640 nm) spectra of **2** (2 μM) upon the addition of AQ (from 0 to 16 μM) in water. (c) Job's plot for determination of the binding stoichiometry between **2** and AQ by monitoring the fluorescence intensity at 732 nm. The total concentration of **1** and AQ was fixed at 10 μM. (d) A Benesi–Hildebrand plot for determination of the binding constant of **2** and AQ.

stimulated emission (SE), while the latter were from the absorptions of the excited singlet state (Figure S10). Based on the decay profile of the band at 694 nm, the lifetime of this species was found to be 1.86 ns. For the tetrakis(β-CD) analogue **2**, its transient absorption spectra were similar to those of **1** (Figure S11). The GSB and SE appeared at 725 nm, which was consistent with the ground-state absorption and fluorescence emission of this compound. Moreover, the excited state absorption band at 600 nm showed little decay within the experimental window compared to the excited singlet state bands at 550 and 1000 nm, which indicated that this band could be from an absorption of the excited triplet state. The decay profile of the GSB/SE was best-fitted with a two-exponential function, giving two lifetimes at 0.48 ps and 1.17 ns, which were found to be much faster than that of the bis(β-CD) counterpart **1**. The faster intersystem crossing for **2** was consistent with the earlier formation of the excited triplet state absorption (at 600 nm) in **2**, which was not the case in **1**.

For ZnTPPS, the transient absorption spectra obtained upon pulse excitation at 550 nm (Figure S12) were similar to those of other zinc(II) porphyrins as reported before.[16] Peaks at 456, 578, and 628 nm were observed, which could be associated with the excited-state absorptions corresponding to $S_1 \rightarrow S_2$, S_3, etc., transitions. Moreover, the GSB signals (550 and 600 nm) and SE (650 nm) aligned perfectly with the Q-band absorptions and fluorescence emission, respectively. In the near-infrared region, the transient absorption spectra showed a band at 1241 nm, which has been previously assigned to the S1 to S2 transition. These singlet excited state features diminished gradually to populate the triplet excited state via intersystem crossing with a set of new bands appearing at 480 and 820 nm. By monitoring the decay of the peak at 1241 nm, the lifetime of the singlet excited state of ZnTPPS was determined to be 1.73 ns. These spectral features were similar to those observed for other zinc(II) porphyrins reported previously.[16]

For the host–guest complex of **1** and ZnTPPS (2:1) in deaerated water, selective excitation of ZnTPPS at 550 nm showed instantaneous formation of spectral features (Figure 7a) similar to those of ZnTPPS in the absence of **1** (Figure S12a). The appearance of ZnTPPS specific excited state features at 460, 560, 625, 830, and 1240 nm and a SE peak at 675 nm in the early time (< 1 ps) confirmed the selective excitation of the donor ZnTPPS. In the next 2 ps, the peak maximum of the SE shifted to 700 nm, indicating the sensitization of **1** by EET as early as 2 ps. Moreover, the broadening of the SE was consistent with the co-existence of excited states of ZnTPPS and **1** in the early time after excitation. At later time (30 ps), the SE peak was sharpened as it lost amplitude in the blue region, which was

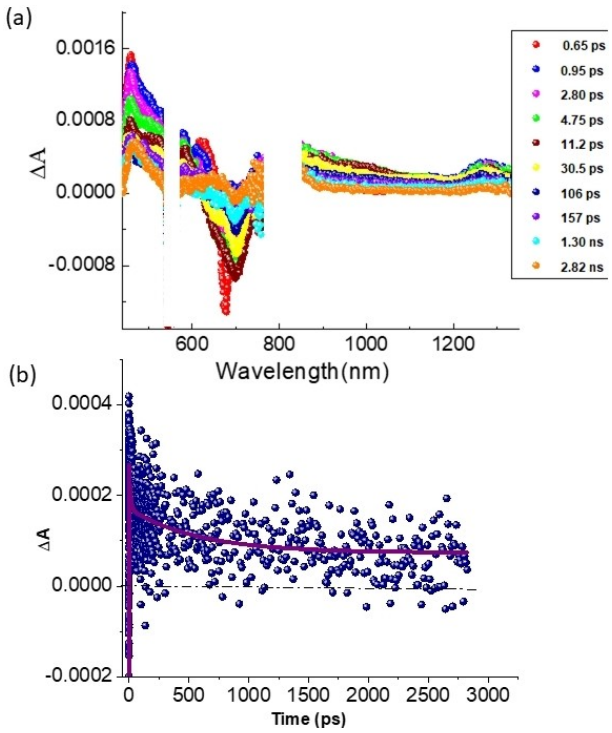

Figure 7. (a) Differential absorption spectra obtained upon femtosecond laser photolysis (λ_{ex} = 550 nm) of a 2:1 mixture of **1** and ZnTPPS in deaerated water at the indicated time intervals. (b) Time profile of the singlet excited state of **1** at 1268 nm.

consistent with the decay of the SE signals from ZnTPPS. Similarly, by this time the ZnTPPS specific visible region excited state features (450–650 nm) lost about 50% amplitude. This observation provided clear evidence for singlet-singlet energy transfer from the photoexcited ZnTPPS to **1**. Assuming energy transfer is the main quenching path, the decay time constant of the near-infrared peak of ZnTPPS in the 1260 nm range corresponding to the singlet-singlet transition was monitored. The decay time constant for this peak of the complex was found to be 583 ps (Figure 7b). Using this time constant and that of the earlier discussed pristine ZnTPPS, rate constant for energy transfer, k_{ENT} ($=1/\tau_{complex}-1/\tau_{ZnTPPS}$), was determined and was found to be $4.88\times10^9\ s^{-1}$, which was two orders of magnitude slower than that of our previously reported covalently linked porphyrin-phthalocyanine conjugates wherein the porphyrin and phthalocyanine units were much close to each other.[17b] Similarly, the energy transfer from the excited ZnTPPS to the tetrakis(β-CD) analogue **2** was also confirmed by the occurrence of a bleaching signal at 725 nm corresponding to the singlet excited state of **2** (Figure S13). Faster decay of the near-infrared peak at 1268 nm was also witnessed, and by fitting, two decay time constants, 445 and 1485 ps were obtained. Using these values and that of pristine ZnTPPS, the k_{ENT} values were determined to be $1.15\times10^9\ s^{-1}$ and $0.11\times10^9\ s^{-1}$, respectively. The bi-exponential decay of the singlet excited state of ZnTPPS suggested the equilibrium existence of different bound forms of the complexes.

The photoinduced processes of a 1:4 mixture of **1** and AQ in deaerated water were then studied similarly. Figure 8a shows the differential absorption spectra of the mixture upon femtosecond laser pulse excitation at 650 nm. Comparing the spectra with those of **1** alone (Figure S10), it was found that the excited-stated absorption of **1** at 495 nm by ca. 1 ns was significantly decayed, and the peak at 800 nm was missing. The decay at 495 nm gave a time constant of 0.44 ns, which was faster than that for **1** alone (1.2 ns) (Figure 8b), indicating the occurrence of an additional photoinduced process in the presence of AQ units. A new transient absorption at 865 nm was also observed, which was a characteristic signal of phthalocyanine radical cations[6a,16a,17] and therefore could be assigned to the radical cation of **1**. The spectrum of $AQ^{\bullet-}$ is expected to appear in the region of 500–600 nm[18] but was buried within the strong excited state absorption peaks of **1**. To provide further evidence and confirm that this peak is from the absorption of the oxidized **1**, the spectrum of **1** was recorded in the presence of nitrosonium tetrafluoroborate, which served as an oxidizing agent. It was found that the radical cation of **1** showed an absorption at 798 nm (Figure S14a). These results indicated the presence of PeT from the excited **1** to the electron acceptor AQ moieties to form a charge-separated state. More-

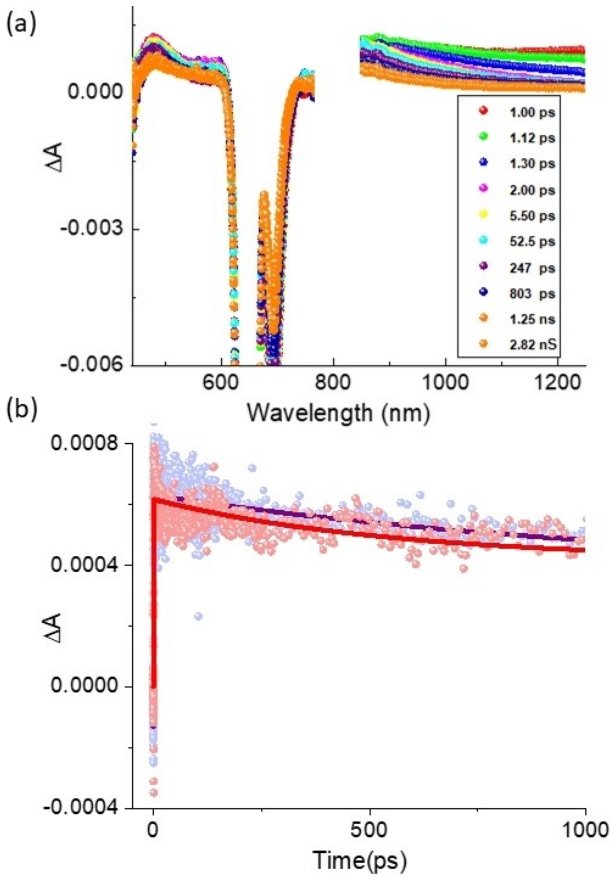

Figure 8. (a) Differential absorption spectra obtained upon femtosecond laser photolysis (λ_{ex} = 650 nm) of a 1:4 mixture of **1** and AQ in deaerated water at the indicated time intervals. (b) Time profile of the singlet excited state of **1** at 495 nm in the absence and presence of AQ.

over, comparing the kinetic traces for **1** and the complex at 495 nm (Figure 8b), the trace for the complex showed a fast decay component, which was missing in the trace for **1** alone. This fast decay in the amplitude of the excited-state absorption of **1** is attributed to the deactivation of the excited state of **1** due to PeT to AQ.

Similar studies were performed for **2** and its 1:8 mixture with AQ (Figures S15 and S14b). From the transient absorption spectra, it can be seen that the transient absorption band due to the radical cation of **2** was also present. Importantly, the lifetime of the excited **2** was shortened from 1.27 ns to 0.11 ns (average) in the presence of AQ.

Finally, the transient absorption spectra of a mixture of **1** (or **2**), ZnTPPS, and AQ were recorded upon femtosecond laser pulse excitation of the porphyrin unit at 550 nm (Figures 9a,b). In both cases, the 1 ps transient absorption spectra showed the features specific for ZnTPPS as discussed above, confirming again the selective excitation of ZnTPPS. In the next 20 ps, the spectra showed a clear growth in the SE of **1** and **2** at 699 and 725 nm assigned to the singlet excited state of **1** and **2**, respectively, while the peak at 465 nm assigned to the excited-state absorption of the donor ZnTPPS showed a concomitant decay. The decay at 465 nm in the ternary complexes containing **1** or **2**, with a time constant of 0.08 ps for both cases, was 5 orders of magnitude faster than that of ZnTPPS alone, which gave a time constant of 2.3 ns (Figures 9c,d). Moreover, the kinetic traces at 465 nm clearly showed that about 85–90% of the amplitude was decayed by about 20 ps. In addition, the weak absorption bands in the region of 750–800 nm indicated a possible population of phthalocyanine radical cations formed by subsequent electron transfer to the AQ units. Unfortunately, these signals were too weak to allow determination of the lifetime of the charge-separated state or the rate of charge separation and recombination.

Conclusion

The host–guest interactions of two water-soluble β-CD-conjugated phthalocyanines (compounds **1** and **2**) and ZnTPPS

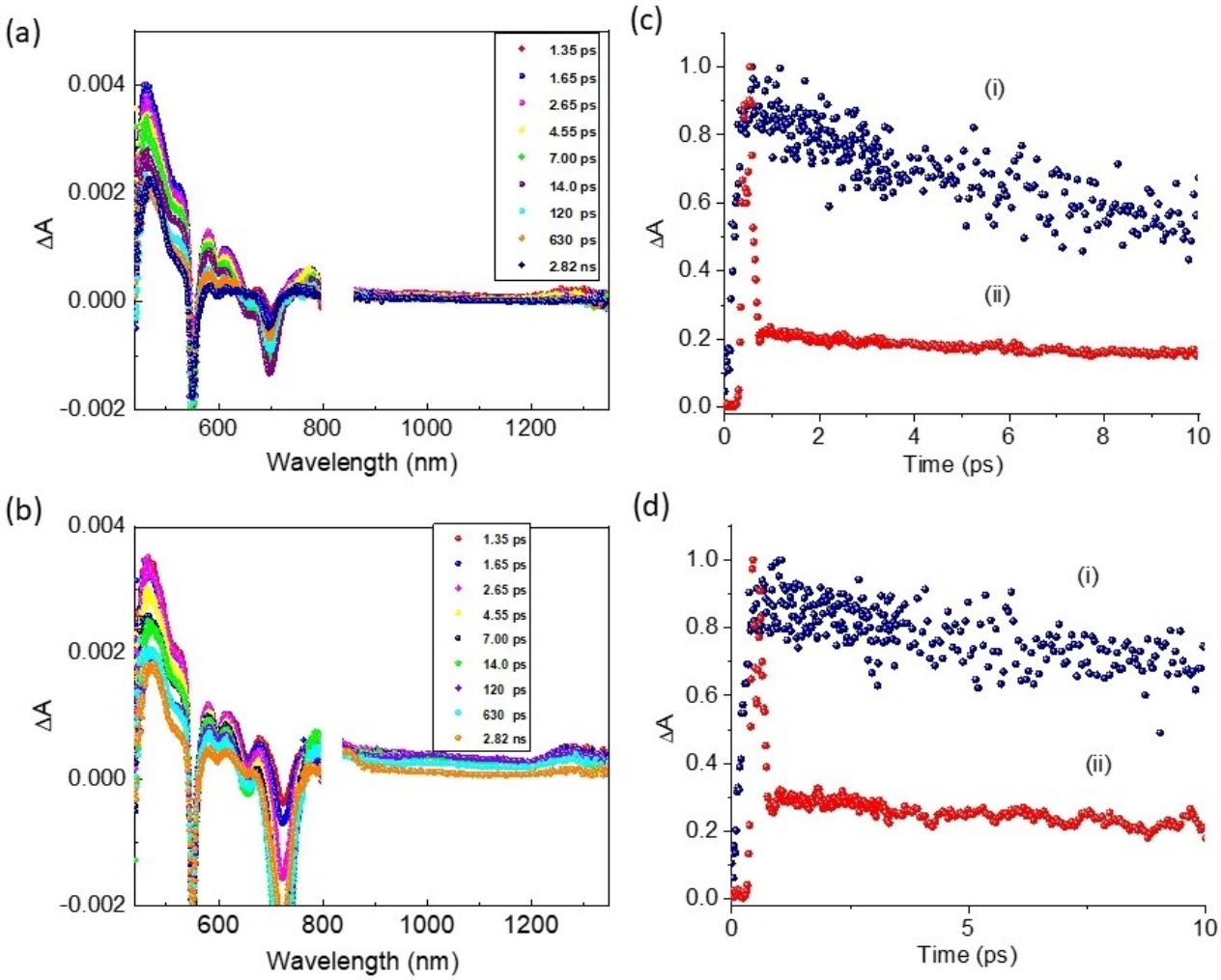

Figure 9. (a) Differential absorption spectra obtained upon femtosecond laser photolysis (λ_{ex} = 550 nm) of a 2:1:4 mixture of **1**, ZnTPPS, and AQ in deaerated water at the indicated time intervals. (b) The corresponding spectra for a 2:1:8 mixture of **2**, ZnTPPS, and AQ. (c and d) Time profile of the singlet excited state of ZnTPPS at 465 nm in the (i) absence and (ii) presence of **1** (or **2**) and AQ.

and/or AQ in water were studied using electronic absorption and fluorescence spectroscopic methods. It was found that these β-CD conjugates formed robust supramolecular arrays with ZnTPPS and AQ in water. For the complexes with the former, EET occurred efficiently, while for the complexes with the latter, PeT was clearly revealed. By assembling the three components together, the resulting ternary complexes could serve as artificial photosynthetic models, for which excitation of the ZnTPPS units resulted in EET to the phthalocyanine core, followed by PeT to the AQ units. These sequential photo-induced processes were further revealed by femtosecond transient absorption spectroscopy, which clearly showed the characteristic signals of phthalocyanine radical cations. However, the lifetime of the charge-separated state was too short to be determined possibly due to the fast charge recombination rate in the polar water solvent and only a small portion of excited phthalocyanines underwent a decay pathway via the PeT process.

Experimental Section

General

Compounds **1** and **2** were prepared according to our previously reported procedure.[10] ZnTPPS and AQ were purchased and used without further purification. Electronic absorption and steady-state fluorescence spectra were recorded on a Gary 5G UV-Vis-NIR spectrophotometer and a Hitachi F-7000 spectrofluorometer, respectively. Fluorescence lifetimes were determined by a time-correlated single-photon counting method on a HORIBA FluoroMax spectrofluorometer with an excitation source at 630 nm. The data were analyzed using the HORIBA decay analysis software.

Determination of the Binding Constant for 1 and AQ

The binding constant for **1** and AQ was determined by a linear least-squares analysis of the fluorescence intensity data using Equation (2) for 1 : 2 host–guest complexes:[13]

$$\frac{[H]_0[G]_0^2}{\Delta I} = \frac{1}{\Delta\varepsilon_a K} + \frac{[G]_0([G]_0 + 4[H]_0)}{\Delta\varepsilon_a} \quad (2)$$

in which $[H]_0$ and $[G]_0$ are the initial concentrations of the host and guest, respectively, and ΔI and $\Delta\varepsilon_a$ denote the changes in the fluorescence and emission coefficient of the host upon complexation with the guest. The binding constant (K) of the complex was determined from the linear plot of $[H]_0[G]_0^2/\Delta I$ against $[G]_0([G]_0 + 4[H]_0)$.

Determination of the Binding Constant for 2 and AQ

The binding constant for **2** and AQ was determined by a modified Benesi–Hildebrand equation of the fluorescence intensity data using Equation (3) for 1 : 4 host–guest complexes:[15]

$$\frac{1}{I - I_0} = \frac{1}{(I_\infty - I_0)K[G]^4} + \frac{1}{I_\infty - I_0} \quad (3)$$

in which I_0 and I are the fluorescence intensity of the host in the absence and presence of the guest, respectively, and I_∞ is the fluorescence intensity of the host when all the host molecules are complexed by the guest molecules. The binding constant (K) of the complex was determined from the linear plot of $1/(I–I_0)$ against $1/[G]^4$.

Femtosecond Transient Absorption Spectroscopic Studies

Experiments were performed using an ultrafast femtosecond laser source (Libra) by Coherent incorporating a diode-pumped, mode-locked Ti:sapphire laser (Vitesse), and a diode-pumped intracavity doubled Nd:YLF laser (Evolution) to generate a compressed laser output of 1.45 W. For optical detection, a Helios transient absorption spectrometer coupled with a femtosecond harmonics generator, both provided by Ultrafast Systems LLC, was used. The sources for the pump and probe pulses were derived from the fundamental output of Libra (Compressed output 1.45 W, pulse width 100 fs) at a repetition rate of 1 kHz; 95 % of the fundamental output of the laser was introduced into a TOPAS-Prime-OPA system with a 290–2600 nm tuning range from Altos Photonics Inc., (Bozeman, MT), while the rest of the output was used for generation of a white light continuum. Kinetic traces at appropriate wavelengths were assembled from the time-resolved spectral data. Data analysis was performed using a Surface Xplorer software supplied by Ultrafast Systems. All measurements were conducted in degassed solutions at 298 K. The estimated error in the reported rate constants is $\pm$10 %.

Acknowledgements

This work was supported by the Research Grants Council of the Hong Kong Special Administrative Region under the Theme-Based Research Scheme (Project No. T23-407/13 N to D.K.P.N.), Guangdong Academy of Sciences (2020GDASYL-20200103045 to X.F.C), and the US-National Science Foundation (2000988 and 1401188 to F.D.).

Conflict of Interests

The authors declare no conflict of interest.

Data Availability Statement

The data that support the findings of this study are available in the supplementary material of this article.

Keywords: cyclodextrins · host–guest interactions · phthalocyanines · photosynthetic models · porphyrins

[1] a) H. Lokstein, G. Renger, J. P. Götze, *Molecules* **2021**, *26*, 3378; b) Y. Shlosberg, G. Schuster, N. Adir, *Front. Plant Sci.* **2022**, *13*, 955843.
[2] a) M. Dokic, H. S. Soo, *Chem. Commun.* **2018**, *54*, 6554–6572; b) A. H. Proppe, Y. C. Li, A. Aspuru-Guzik, C. P. Berlinguette, C. J. Chang, R. Cogdell, A. G. Doyle, J. Flick, N. M. Gabor, R. van Grondelle, S. Hammes-Schiffer, S. A. Jaffer, S. O. Kelley, M. Leclerc, K. Leo, T. E. Mallouk, P. Narang, G. S. Schlau-Cohen, G. D. Scholes, A. Vojvodic, V. W.-W. Yam, J. Y. Yang, E. H. Sargent, *Nat. Rev. Mater.* **2020**, *5*, 828–846; c) Z. Wang, Y.

Hu, S. Zhang, Y. Sun, *Chem. Soc. Rev.* **2022**, *51*, 6704–6737; d) L. Yang, D. Fan, Z. Li, Y. Cheng, X. Yang, T. Zhang, *Adv. Sustainable Syst.* **2022**, *6*, 2100477.
[3] a) D. K. Dogutan, D. G. Nocera, *Acc. Chem. Res.* **2019**, *52*, 3143–3148; b) E. A. R. Cruz, D. Nishiori, B. L. Wadsworth, N. P. Nguyen, L. K. Hensleigh, D. Khusnutdinova, A. M. Beiler, G. F. Moore, *Chem. Rev.* **2022**, *122*, 16051–16109.
[4] a) G. Bottari, O. Trukhina, M. Ince, T. Torres, *Coord. Chem. Rev.* **2012**, *256*, 2453–2477; b) M. E. El-Khouly, S. Fukuzumi, F. D'Souza, *ChemPhysChem* **2014**, *15*, 30–47; c) J. D. Megiatto Jr, D. M. Guldi, D. I. Schuster, *Chem. Soc. Rev.* **2020**, *49*, 8–20; d) S. Fukuzumi, Y. M. Lee, W. Nam, *J. Porphyrins Phthalocyanines* **2020**, *24*, 21–32; e) E. Nikoloudakis, I. López-Duarte, G. Charalambidis, K. Ladomenou, M. Ince, A. G. Coutsolelos, *Chem. Soc. Rev.* **2022**, *51*, 6965–7045; f) H. Jing, J. Rong, M. Taniguchi, J. S. Lindsey, *Coord. Chem. Rev.* **2022**, *456*, 214278.
[5] a) M. G. Walter, A. B. Rudine, C. C. Wamser, *J. Porphyrins Phthalocyanines* **2010**, *14*, 759–792; b) C. Wang, M. P. O'Hagan, B. Willner, I. Willner, *Chem. Eur. J.* **2022**, *28*, e202103595; c) B. Gibbons, M. Cai, A. J. Morris, *J. Am. Chem. Soc.* **2022**, *144*, 17723–17736; d) A. Kobayashi, S.-y. Takizawa, M. Hirahara, *Coord. Chem. Rev.* **2022**, *467*, 214624.
[6] a) X.-F. Chen, M. E. El-Khouly, K. Ohkubo, S. Fukuzumi, D. K. P. Ng, *Chem. Eur. J.* **2018**, *24*, 3862–3872; b) E. Anaya-Plaza, J. Joseph, S. Bauroth, M. Wagner, C. Dolle, M. Sekita, F. Gröhn, E. Spiecker, T. Clark, A. de la Escosura, D. M. Guldi, T. Torres, *Angew. Chem. Int. Ed.* **2020**, *59*, 18786–18794; *Angew. Chem.* **2020**, *132*, 18946–18955; c) R. J. M. Nolte, *J. Porphyrins Phthalocyanines* **2020**, *24*, 1243–1257.
[7] a) E. A. Ermilov, S. Tannert, T. Werncke, M. T. M. Choi, D. K. P. Ng, B. Röder, *Chem. Phys.* **2006**, *328*, 428–437; b) S. Tannert, E. A. Ermilov, J. O. Vogel, M. T. M. Choi, D. K. P. Ng, B. Röder, *J. Phys. Chem. B* **2007**, *111*, 8053–8062.
[8] a) X. Leng, C.-F. Choi, P.-C. Lo, D. K. P. Ng, *Org. Lett.* **2007**, *9*, 231–234; b) X. Leng, D. K. P. Ng, *Eur. J. Inorg. Chem.* **2007**, *2007*, 4615–4620; c) E. A. Ermilov, R. Menting, J. T. F. Lau, X. Leng, B. Röder, D. K. P. Ng, *Phys. Chem. Chem. Phys.* **2011**, *13*, 17633–17641; d) R. Menting, J. T. F. Lau, H. Xu, D. K. P. Ng, B. Röder, E. A. Ermilov, *Chem. Commun.* **2012**, *48*, 4597–4599; e) R. Menting, D. K. P. Ng, B. Röder, E. A. Ermilov, *Phys. Chem. Chem. Phys.* **2012**, *14*, 14573–14584.
[9] a) K. Wang, K. Velmurugan, B. Li, X.-Y. Hu, *Chem. Commun.* **2021**, *57*, 13641–13654; b) M. E. El-Khouly, A. M. Kobaisy, G. Sallam, M. Yoshihisa, *J. Porphyrins Phthalocyanines* **2022**, *26*, 132–139.
[10] X.-F. Chen, D. K. P. Ng, *Chem. Commun.* **2021**, *57*, 3567–3570.
[11] a) J. S. Manka, D. S. Lawrence, *J. Am. Chem. Soc.* **1990**, *112*, 2440–2442; b) K. Kano, R. Nishiyabu, T. Asada, Y. Kuroda, *J. Am. Chem. Soc.* **2002**, *124*, 9937–9944.
[12] K. Sasaki, H. Nakagawa, X. Zhang, S. Sakurai, K. Kano, Y. Kuroda, *Chem. Commun.* **2004**, 408–409.
[13] Y. Liu, H.-M. Yu, Y. Chen, Y.-L. Zhao, *Chem. Eur. J.* **2006**, *12*, 3858–3868.
[14] Y. Kuroda, M. Ito, T. Sera, H. Ogoshi, *J. Am. Chem. Soc.* **1993**, *115*, 7003–7004.
[15] J. Mohanty, A. C. Bhasikuttan, S. D. Choudhury, H. Pal, *J. Phys. Chem. B* **2008**, *112*, 10782–10785.
[16] a) S. K. Das, A. Mahler, A. K. Wilson, F. D'Souza, *ChemPhysChem* **2014**, *15*, 2462–2472; b) S. K. Das, B. Song, A. Mahler, V. N. Nesterov, A. K. Wilson, O. Ito, F. D'Souza, *J. Phys. Chem. C* **2014**, *118*, 3994–4006.
[17] a) M. E. El-Khouly, S. Fukuzumi, *J. Porphyrins Phthalocyanines* **2011**, *15*, 111–117; b) C. B. KC, G. N. Lim, P. A. Karr, F. D'Souza, *Chem. Eur. J.* **2014**, *20*, 7725–7735.
[18] M. Fujita, A. Ishida, T. Majima, S. Takamuku, *J. Phys. Chem.* **1996**, *100*, 5382–5387.

Manuscript received: March 5, 2023
Accepted manuscript online: March 29, 2023
Version of record online: May 5, 2023